Geochemical Perspectives Letters

Unravelling the controls on the molybdenum isotope ratios of river waters

K. Horan, R.G. Hilton, A.J. McCoy-West, D. Selby, E.T. Tipper, S. Hawley, K.W. Burton

Supplementary Information

The Supplementary Information includes:

- 1. Sampling Locations
- 2. Sampling Methods
- 3. Analytical Methods
- 4. Supplementary Discussion of Soil and Suspended Sediment $\delta^{98/95}$Mo Values
- 5. Quantifying Mo Removal from Solution and the Mo Fractionation Model
- Tables S-1 to S-5
- Figures S-1 to S-6
- Supplementary Information References

1. Sampling Locations

1.1 New Zealand

The Southern Alps is a steep mountain belt built by transpression along the Alpine Fault and it has an uplift rate of 8–10 mm yr^{-1} (Tippett and Kamp, 1995). The western flank has a temperate climate, with a high erosion rate driven by orographic precipitation, exceeding 8 m yr^{-1}, steep slopes and bedrock landslides that expose meta-sedimentary rocks (Hovius *et al.*, 1997; Jacobson *et al.*, 2003). Along the western Southern Alps, the metamorphic grade varies perpendicular to the Alpine Fault strike, but the sedimentary protolith is similar in all catchments and the organic carbon content of the rocks ranges from ~0.1 to 0.2 % (Horan *et al.*, 2017). Physical erosion yields vary from 4072 t km^{-2} yr^{-1} to 10,136 t km^{-2} yr^{-1} (Hicks *et al.*, 2011). Chemical denudation yields range from 110 t km^{-2} yr^{-1} to 120 t km^{-2} yr^{-1} (Jacobson and Blum, 2003) and oxidative weathering fluxes are high (Horan *et al.*, 2017). The extent of weathering, as quantified by the chemical denudation yield over the total (chemical + physical) denuation, W/D, is ~0.03 to 0.01. River samples were collected from 11 major catchments in the western Southern Alps and two draining the eastern flank (Fig. S-1; Tables S-1–S-4).

1.2 Mackenzie River Basin and Yukon River

The Mackenzie River Basin spans a large area of 1.78×10^6 km^2 and drains the Rocky and Mackenzie Mountains (Rockies) in north west Canada. The basin geology is dominated by sedimentary rocks (clastics and carbonates), including the carbonate platform in the central part, the carbonaceous shales of the interior plain and the Rockies, which are mainly composed of carbonate, dolomitic

limestone and shale (Calmels *et al*., 2007; Millot *et al*., 2003). The sedimentary rocks host organic carbon, with concentrations that are typically between 0.1 and 0.3 wt. % organic carbon (OC), but can reach 0.6 wt. % locally in the Peel catchment (Hilton *et al*., 2015). Black shales outcrop in parts of the Mackenzie Mountains that drain to the upper part of the basin (Johnston *et al*., 2012). Five key localities from the basin were included in the Mo isotope analysis. Two sampling localities were along the main channel of the Mackenzie River, at the Environment Canada gauging stations Tsiigehtchic and the Middle Delta (Horan *et al*., 2019). In addition, the Peel River and its tributary, the Ogilvie River, which join the Mackenzie River between Tsiigetchic and the Middle Delta were assessed (Table S-1–S-3). The Yukon River was sampled at Dawson to the south west of Mackenzie River Basin. The average annual suspended sediment yields for the Mackenzie (Tsiigetchic) and Peel are 124 t km^{-2} yr^{-1} and 294 t km^{-2} yr^{-1}, respectively (Carson and Conly, 1998). Chemical denudation rates are ~8–20 t km^{-2} yr^{-1} (Millot *et al*., 2003) and W/D ~0.06; which is higher than that in the western Southern Alps.

1.3 Iceland

In Iceland, sampling focussed on the Skaftá River catchment, which drains the Skaftárjökull area of the Vatnajökull glacier in the south of the island (Fig. S-2). Although this region is predominantly basaltic, the Skaftá River is sourced directly from the Vatnajökull glacier, which covers sulfide bearing rocks from the tholeiitic rock suite (Jónsdóttir, 2008; Torssander, 1989). Bedrock ages here range from Quaternary to Recent. Average physical erosion rates are ~2084 t km^{-2} yr^{-1} and the average chemical weathering rates are 50 t km^{-2} yr^{-1}, with W/D ~0.02 (Gislason *et al*., 1996; Pogge von Strandmann *et al*., 2006)

2. Sampling methods

2.1 River water

In the Southern Alps, river waters were collected from the centre of river channels at their surface. Catchments were sampled 2–6 times over a 1 month period (14/09/14–03/10/14) under different discharge regimes. Each water sample (7–8 litres) was transferred into a clean bucket and decanted to sterile plastic bags. The sample bags were weighed to determine the sample volume, prior to water filtration through 142 mm diameter, 0.2 μm polyethersulfone (PES) filters in pre-cleaned filter units within a day of collection. Samples were stored in acid-cleaned low-density polyethylene (LDPE) bottles in the dark at 4 °C. All water samples intended for cation and trace metal analysis were acidified in the field to pH ~2 following published methods (Dalai *et al*., 2002; Hilton *et al*., 2014) with an un-acidified aliquot kept for anion analyses. Details of this sample set can be found in Horan *et al*. (2017). Out of the sample set, 13 samples from the major rivers draining the western Southern Alps and 3 from the eastern Southern Alps were selected for Mo isotope analysis (Table S-3). Two 250 mL rainwater samples were collected from the Franz Josef area over separate 10 h periods to evaluate the potential atmospheric contribution of Mo to the river waters. Similar methods were used to collect and process water samples from the Mackenzie River Basin in 2013 and the Skaftá River catchment in 2013 and 2014.

We did not analyse a time-series of samples for their dissolved Mo isotope ratios. Ideally, it would be beneficial to collect river water samples across different flow events, thereby capturing water from different flow pathways and allowing flux-weighted average Mo isotope ratios to be determined (King and Pett-Ridge, 2018). In the absence of this information, we do not quantify Mo fluxes or flux-weighted averages and focus on seeking to explain the differences between indivdiual samples.

2.2 Soils, river bed materials and river suspended loads

Surface soils and weathered colluvium samples were collected from the western Southern Alps, as described by Horan *et al*. (2017). In summary, we measured the Mo isotope ratios in surface soils through to more weathered colluvium on the forested hillslopes of Alex Knob, which drains to the Doherty Creek catchment. Four ~500 cm^3 sized samples of weathered colluvium from 10 to 70 cm depth below the soil surface were collected at three sites (Table S-4).

To help constrain the composition of the parent materials undergoing weathering, the least weathered portion of the river load, the river bed material, was sampled from the Southern Alps and the Mackenzie Basin (*e.g.,* Hilton *et al*., 2010; Dellinger *et al*., 2014; Horan *et al*., 2017) (Table S-1). In summary, in New Zealand, samples were collected from channel edges or from bank deposits that represent the fine fraction deposited during high flow regimes and transferred to sterile plastic bags. In the Mackenzie Basin, samples were collected from the river bed using a metal bucket as a dredge (Hilton *et al*., 2015). In Iceland, we use published data from basaltic rock samples (Yang *et al*., 2015) to constrain the composition of Mo in the parent materials.

In addition, suspended sediments were collected in New Zealand and Canada (Table S-2). These contain a mixture of the signature of unweathered rocks, together with solid products of modern weathering processes (Dellinger *et al*., 2014). Suspended sediment was immediately rinsed from the 0.2 μm filter surface using filtered river water and transferred to clean amber-glass vials. All suspended sediments were freeze-dried upon return to laboratories within two weeks and weighed.

3. Analytical methods

3.1. Mo concentration and isotope ratios

Molybdenum measurements were performed in the Arthur Holmes Geochemistry Labs at Durham University following established protocols (Neely *et al*., 2018; Li *et al*., 2019; McCoy-West *et al*. 2019). For river waters, Mo concentrations were first measured by direct calibration against a pure Mo standard by quadrupole inductively coupled mass spectrometry (Q-ICP-MS, X-Series). This was used to obtain preliminary Mo concentrations and allow spiking at the ideal spike to sample ratio. Dissolved Mo was then separated and purified using anion exchange chromatography. Depending on the Mo concentration, between 30 and 500 mL of the water was doped with a known amount of a ^{97}Mo-^{100}Mo double spike solution to achieve a combined Mo mass of ~100 ng and a spike-sample mix ratio of 1:1. The chemistry was modified from that described by Pearce *et al*. (2009). The spiked water sample was evaporated to dryness before being re-dissolved in 5 mL 0.5M HCl for loading on to 2 mL of anion exchange resin (Bio-Rad AG1-X8) in a column. The resin was pre-cleaned with 20 mL 8M HNO_3, 10 mL 6M HCl, 10 mL 1M HCL, 5 mL 1M HF and 10 mL 3M HNO_3, and preconditioned with 5 mL 0.5M HCl. The sample was loaded on to the anion exchange resin in 5 mL 0.5M HCl, and the bulk matrix was washed through with 5 mL 0.5M HCl, 10 mL 0.5M HCl + 1M HF, 8 mL 4M HCl and 12 mL 1M HF. The Mo was finally eluted in 12 mL 3M HNO_3.

For solid samples, sediments were first powdered using a zirconium disc mill, before ~200 mg of sample was digested in a 2:1 mix of concentrated HF-HNO_3 (6 mL total) for 72 hours at 120°C and then evaporated. The dried sample was further digested in a 2:1 mix of concentrated HNO_3-HCl (4.5 mL) for 48 h at 120°C, and then evaporated. Next, 3 mL of 16M HNO_3 followed by 5 mL of 6M HCl was added until the sample was complete dissolved. After this solution was evaporated, the residue was re-dissolved in 10 ml of 1M HCl and a small aliquot (0.5 mL) was extracted for concentration analysis. These initial Mo concentration measurements were acquired on the Q-ICP-MS at Durham University and were used to calculate the ideal spike volume required for $\delta^{98/95}$Mo analysis (based on a 1:1 spike-sample ratio). The subsequent chemistry was based on the method of Willbold *et al*. (2016). The columns were pre-cleaned with 10 mL 0.5M HCl, 10 mL 2M NH_4NO_3 +2M NH_4OH, 10 mL 8M HNO_3, 5 mL 1M HF and 10 mL 0.5M HCl. The columns were then preconditioned in 3 mL 3M HCl. After concentration checks via Q-ICP-MS, the remaining 1M HCl solution from the digestion process was spiked, before being evaporated and brought up in 4.75 mL of 3M HCl for loading. Immediately prior to loading, 0.25 mL of ascorbic acid was also added to the samples to oxidise Fe from Fe^{2+} to Fe^{3+} and enhance removal of Fe adsorbed to the resin matrix. The volume of anion exchange resin used was 1 mL. A bulk wash with 3 mL 3M HCL followed. A 13 mL mixture consisting of 0.5M + 0.5 % H_2O_2 was then added to the columns in 1 mL aliquots for the first 3 mL, and 5 mL aliquots for the final 10 mL, to elute residual Fe. Zinc was eluted in 10 mL 1M HF. The Mo aliquot was collected in 12 mL of 1M HCl in acid cleaned Teflon beakers. The total procedural blanks for processing Mo in this study ranged from 0.1–1.7 ppb, with a mean blank [Mo] = 0.75±0.51 ppb (n = 16, ±1SD).

Isotope measurements were made using a MC-ICP-MS (Thermo-Fischer Neptune) in the Arthur Holmes Geochemistry Laboratories, Durham University. Samples were introduced to the instrument using an Aridus II desolvator and a Savillex PFA20 nebuliser at 150–200 ppb concentration in 0.5M HNO_3. The data were deconvolved using IsoSpike (Creech *et al*. 2015), which is an add-in to the Iolite software package. Data are presented in delta notation ($\delta^{98/95}$Mo), reported relative to the NIST-SRM-3134 standard reference material (SRM) (Eq. S-1), where $\delta^{98/95}Mo_{NIST\text{-}3134}$ = 0 ‰.

$$\delta^{98}\mathrm{Mo} = \left[\left(\frac{\left({}^{98}Mo/{}^{95}Mo\right)_{sample}}{\left({}^{98}Mo/{}^{95}Mo\right)_{NIST-SRM-3134}}\right) - 1\right] \times 1000\ [‰] \qquad \text{Eq. S-1}$$

3.2 Precision and Accuracy

The long-term $\delta^{98/95}$Mo machine reproducibility was determined by measurement of an in-house Romil standard run under the same instrumental conditions, which gave $\delta^{98/95}$Mo = 0.046±0.029 ‰ (n = 99, ±2 SD) in agreement with other studies (Neely *et al*., 2018; Li *et al*., 2019; McCoy-West *et al*., 2019). The long-term reproducibility of international reference materials is presented in Figure S-3. The average value of the IAPSO seawater reference material is $\delta^{98/95}$Mo = 2.07±0.06 ‰ (n = 5, ±2 SD), which is indistinguishable from the mean of published values of 2.08±0.10 ‰ (Goldberg *et al*., 2013). The average composition of USGS rock standard BHVO-1 obtained here is $\delta^{98/95}$Mo = -0.19±0.04 ‰ (n = 21, ±2 SD, Table S-5), which is within uncertainty of previous determinations (*e.g.* McCoy-West *et al*., 2019). Overall, replicate concentration analyses on the standards IAPSO and BHVO-1 by isotope dilution methods produced data in agreement to within 8 and 4 %, respectively. For concentrations, the IAPSO standard measured by ID MC-ICP-MS yielded a concentration of 10.9±0.51 ppb (n = 5, ±2 SE, Table S-5), in agreement with published values of 10 and 11 ppb (Greber *et al*., 2012).

Duplicate sample data are provided in the data tables. Full procedural duplicate analyses on two water samples produced data in agreement to within 0.04 ‰ and these data were averaged and reported with ±2 SD error on the mean value. Duplicate

analyses on 12 sediment samples produced data in agreement to within 0.1 ‰, with a mean difference of 0.03 ‰. Sample reproducibility for solid samples shows that analyses are within the ±2 SD error of the 0.05 ‰ fits to a 1:1 line (Fig. S-4).

3.3 A note on reporting Mo isotope ratios

After almost two decades of development of the Mo isotope system (Kendall *et al*., 2017), the international standard NIST-SRM-3134 is now recommended for $\delta^{98/95}$Mo measurements (Goldberg *et al*., 2013) and is widely used for Mo isotope measurements (*e.g.*, Wang *et al*., 2015; King *et al*., 2016; Neely *et al*., 2018). However, a large amount of published data that derived from groups who pioneered the Mo isotope measurement were normalised relative to reference materials that were broadly similar, but had important differences (Kendall *et al*., 2017). In general, the Mo in these reference materials was isotopically lighter than NIST-SRM-3134 (Goldberg *et al*., 2013; Nägler *et al*., 2014).

Goldberg *et al*. (2013) undertook a cross-laboratory calibration of these internal laboratory standards used in the vast majority of published studies. These measurements were made relative to NIST-SRM-3134 as per Eq. S-1. The differences between the internal laboratory standards and NIST-SRM-3134 varied from -0.16 ‰ to -0.37 ‰.

Some studies have used Goldberg *et al*. (2013) correction factors to compare new measurements made relative to NIST-SRM-3134 to published data using other reference materials (*e.g.*, Yang *et al*., 2015). In contrast, Nägler *et al*., (2014) suggested that data measured relative to NIST-SRM-3134 should be shifted by a nominal value (0.25 ‰), based on the average from the Goldberg *et al*., (2013) paper:

$$\delta^{98}\mathrm{Mo} = \left[\left(\frac{\left({}^{98}Mo/{}^{95}Mo\right)_{sample}}{\left({}^{98}Mo/{}^{95}Mo\right)_{NIST-3134}}\right) - 1\right] \times 1000\ [‰] + 0.25 \qquad \text{Eq. S-2}$$

This approach has been adopted by some (*e.g.*, Neely *et al*., 2018; King and Pett-Ridge, 2018).

Here, we report all our data using Eq. S-1, where NIST3134 = 0 ‰. This has become the accepted norm in high temperature Mo isotope studies (*e.g.*, Yang *et al*., 2015; Bezard *et al*., 2016; Willbold and Elliot, 2017; Li *et al*., 2019; McCoy-West *et al*., 2019) and many low temperature studies (*e.g.*, Siebert *et al*., 2015; King *et al*., 2016, 2018) because, as per definition, a reference material should have a composition of 0 ‰. To compare to published measurements, we identify the standard that was used, and apply a correction based on Goldberg *et al*. (2013) to that data. This accounts for the fact that some internal reference materials are subtly different. For completeness, we provide all this information for a compilation of river, stream and groundwater measurements in Supplementary Table S-6.

3.4 Additional measurements

Rhenium (Re) concentration measurements in waters and solids were determined as outlined in Horan *et al*. (2017). New Zealand measurements are from Horan *et al*. (2017) and Mackenzie River measurements are from Horan *et al*. (2019). Major ion concentrations in water samples were analyzed by Ion Chromatography (Thermo Scientific Dionex) at the Department of Geography, Durham University. Cation and anion standards and a certified reference standard (Lethbridge-03) were run to validate the analytical results. Data on the Re composition of the dissolved load and solid products were determined by isotope dilution coupled to analysis by Q-ICP-MS (Thermo Scientific X-Series) (Horan *et al*., 2017) and are included for comparison to the behaviour of Mo. In river bed materials and soils, the total organic carbon concentration ([OC], %) was measured following a 0.2M HCl leach protocol (Galy *et al*., 2007). Aliquots of samples were combusted and the concentration and stable isotope composition of OC (δ^{13}C, ‰) was determined using a Costech elemental analyser coupled to a Thermo Scientific Delta V Advantage isotope ratio mass spectrometer (EA-IRMS) at Durham University.

4. Supplementary Discussion of Soil and Suspended Sediment $\delta^{98/95}$Mo Values

4.1 Potential inputs of Mo from precipitation to soil in the western Southern Alps

The retention of Mo in the soil materials and potential mechanisms for this are discussed in the main text. Here, we provide supplementary discussion of the potential inputs of Mo from rainfall. Atmospheric inputs can influence soil chemical budgets (Kennedy *et al*., 1998) and soil profiles developed on basaltic bedrock in Hawaii have atmospheric inputs of Mo from volcanic aerosols and/or ash and precipitation (and potentially anthropogenic sources) that play a role in setting the Mo mass budget and isotope signature of soil, especially in older and wetter soils (King *et al*., 2016; Siebert *et al*. 2015). In the western Southern Alps, the mean annual precipitation is high, at ~4–6 m yr^{-1} along the range front (Henderson and Thompson, 1999), but the measured [Mo] (based on Q-ICP-MS) was <0.1 nmol L^{-1} in two rainwater samples; this equates to a precipitation input of ~3–6 × 10^{-5} g yr^{-1} of Mo. In

contrast, physical and chemical denudation in this setting supply ~10 mm yr^{-1} of rock mass to the surface (Hicks *et al*., 2011; Jacobson *et al*., 2003) with a [Mo] = 0.29 ppm, which equates to ~700 × 10^{-5} g yr^{-1} of Mo. From this simplified mass balance, it appears as though Mo inputs from the atmosphere are <1 % in this setting. In Iceland, an input of volcanic ash may affect the Mo content of the soils (*e.g*., King *et al*., 2016). However, ash may not necessarily alter $\delta^{98/95}$Mo values relative to underlying parent material if it has a similar chemical composition (Moune *et al*., 2012; Siebert *et al*., 2015).

4.2 River suspended load

Depending on the physical erosion rate and mechanism (*e.g*., shallow versus deep erosion processes), river suspended sediments can reflect a mixture of weathered and un-weathered materials (Dellinger *et al*., 2014). For Mo, suspended sediments may also be sites of adsorption during fluvial transport, although this has been ruled out in some previous studies (Wang *et al*., 2015). Suspended load in the western Southern Alps and Mackenzie Basin have Mo concentrations that are generally higher than those in the river bed materials (Table S-2). This could reflect hydrodynamic sorting and depletion of felsic minerals such as quartz from the fine suspended load, which acts to increase many element concentrations (*e.g*., Dellinger *et al*., 2014). However, in both settings, the $\delta^{98/95}$Mo values of suspended load are similar to the river bed materials (Tables S-1 and S-2). This suggests that Mo in secondary minerals do not dominate the total mass balance of exported dissolved and particulate Mo fluxes.

5. Quantifying Mo Removal from Solution and the Mo Fractionation Model

The extent of Mo removal from solution during chemical weathering was quantified using the ratio of Mo to Re in the dissolved load relative to the parent materials (Equation 1). This is analogous to tracking the removal of Li to secondary phases by comparing Li to the mobile, soluble element Na (*e.g*., Dellinger *et al*., 2015). The approach assumes stoichiometric release of Re and Mo during weathering and that Re remains in solution at a range of pH and Eh values typical of soils and river waters (Brookins, 1986), whereas Mo is susceptible to uptake to secondary phases (Goldberg *et al*., 1996).

To constrain the [Mo]/[Re] in parent materials, in the western Southern Alps we use the average composition of the sampled river bed materials. This is because lithological variability is relatively minor along strike of the Alpine Fault (Hilton *et al*., 2008; Mortimer 2004) and these bed materials help to provide an integrated perspective of the composition of average sediments eroded from the catchments. In contrast, the larger rivers of the Mackenzie River Basin integrate over larger source areas. Therefore, we use the individual catchment river bed materials for this setting, because lithology is more variable across the different catchments (Beaulieu *et al*., 2011). We take the same approach for the $\delta^{98/95}Mo_{BM}$ values in the analysis (Fig. 3). For the western Southern Alps, this is the average of the river bed materials across the sample set. For the Mackenzie Basin, we pair the individual river bed material sample to the dissolved load sample from the same location (Tables S-1 and S-3).

We model fMo_{diss} and $\Delta^{98/95}Mo_{diss\text{-}BM}$ (the difference between river water, $\delta^{98/95}Mo_{diss}$, and river bed materials $\delta^{98/95}Mo_{BM}$). In the mass balance model, the weathering zone is considered to be an open flow-through system over which Mo is released in dissolved form during the dissolution of primary minerals and removed from solution by incorporation into secondary minerals. At steady state, all of the dissolution and precipitation input and output fluxes are balanced, fMo_{diss} <1 and the Mo isotope ratios of the dissolved phase may be modelled following the method of Bouchez *et al*. (2013):

$$\delta^{98/95}Mo_{diss} = \delta^{98/95}Mo_{rock} - \Delta^{98/95}Mo_{sec\text{-}diss} \times (1 - fMo_{diss}) \qquad \text{Eq. S-3}$$

where $\delta^{98/95}Mo_{rock}$ is the Mo isotope ratios of the rock undergoing weathering and $\Delta^{98/95}Mo_{sec\text{-}diss}$ is the isotope fractionation factor between secondary products and the dissolved load:

$$\Delta^{98/95}Mo_{sec\text{-}diss} = \delta^{98}Mo_{sec} - \delta^{98}Mo_{diss} \qquad \text{Eq. S-4}$$

where $\delta^{98/95}Mo_{sec}$ corresponds to the Mo isotope ratios of the solid weathering products and $\alpha_{sec\text{-}diss}$ is the fractionation factor (Barling and Anbar, 2004). Equation S-3 can be re-written in terms of the difference in the isotope ratios between the rocks and the dissolved phase:

$$\delta^{98/95}Mo_{diss} - \delta^{98/95}Mo_{rock} = -\Delta^{98/95}Mo_{sec\text{-}diss} \times (1 - fMo_{diss}) \qquad \text{Eq. S-5}$$

Here, for the western Southern Alps and Mackenzie Basin, we assume that $\delta^{98/95}Mo_{diss} - \delta^{98/95}Mo_{rock} = \delta^{98/95}Mo_{diss} - \delta^{98/95}Mo_{BM} = \Delta^{98/95}Mo_{diss\text{-}BM}$.

To explore the range of predicted $\Delta^{98/95}Mo_{diss\text{-}BM}$ values as a function of fMo_{diss}, values of $\Delta^{98/95}Mo_{sec\text{-}diss}$ are taken from the experimental data of Goldberg *et al*. (2009) and Barling and Anbar (2004). These range from –0.8 ‰ to –1.4 ‰ for adsorption on to

magnetite through to goethite (Goldberg *et al*. 2009). Fractionation factors for the adsorption of Mo to organic substances are in a similar range (King *et al*., 2018). We find that the modelled batch fractionation factors can explain the majority of the variability in the $f\mathrm{Mo}_{\mathrm{diss}}$ and $\Delta^{98/95}\mathrm{Mo}_{\mathrm{diss\text{-}BM}}$ values of the rivers in our study locations.

The degree of Mo adsorption onto Mn and Fe (oxyhydr)oxides is thought to be strongly pH-dependent (Kim and Zeitlin, 1968), and is limited at pH values >6.5. Between pH values 3–5, Mo may be strongly adsorbed to Fe, Mn, and aluminium (Al) oxides (Goldberg *et al*., 2002; Goldberg and Forster, 1998; Karimian and Cox, 1979; King *et al*., 2018), but at higher pH values, Mo solubility increases and there is decreased adsorption. The latter is associated with increased Mo loss as the soluble molybdate (MoO_4^{2-}). The river waters in New Zealand, Canada and Iceland had pH values mostly between 7 and 8.5 at the time of sampling (Table S-3). This indicates that Mo adsorption to (oxyhydr)oxides may be limited during river transport. This is especially true in New Zealand where the water transport lengths are relatively short (<20 km). However, porewater within soils is expected to have a greater concentration of CO_2 species from soil respiration and therefore lower pH values than water exposed to the atmosphere. Thus, the greatest adsorption of Mo should take place in these lower pH waters. This is consistent with the weathered mineral soil samples from the western Southern Alps (Fig. S-5, Table S-4). Fractionations between the solid and dissolved phase also vary with mineralogy, increasing in the order magnetite ($\Delta^{98/95}\mathrm{Mo}_{\mathrm{diss\text{-}adsorbed}}$ = 0.83±0.60 ‰) < ferrihydrite ($\Delta^{98/95}\mathrm{Mo}_{\mathrm{diss\text{-}adsorbed}}$ = 1.11±0.15 ‰) < goethite ($\Delta^{98/95}\mathrm{Mo}_{\mathrm{diss\text{-}adsorbed}}$ = 1.40±0.48 ‰) < hematite ($\Delta^{98/95}\mathrm{Mo}_{\mathrm{diss\text{-}adsorbed}}$ = 2.19±0.54 ‰) (Goldberg *et al*., 2009). The adsorption of light Mo to Mn and Fe (oxyhydr)oxides in the soils of the river catchments would result in the soil porewaters becoming enriched in the heavier isotopes of Mo (*i.e*. ^{98}Mo), which will subsequently be transferred to the river waters.

There are outliers in $f\mathrm{Mo}_{\mathrm{diss}}$ versus $\Delta^{98/95}\mathrm{Mo}_{\mathrm{diss\text{-}BM}}$ space that cannot be explained by the simple model. Two samples from the Southern Alps, have values of $f\mathrm{Mo}_{\mathrm{diss}}$ that exceed 1, implying this river is gaining Mo relative to Re. This could reflect non-steady state cycling of Mo in the biosphere. Molybdenum is an essential biological micronutrient that is harvested by biological matter for enzyme manufacture. Leaching of the biospheric Mo reservoir to the river waters could drive a transient deviation from steady state mass balance in the river catchment, provided that the rate of Mo addition exceeds the rate of Mo adsorption to Fe and Mn oxy(hydroxides) in the deeper soil horizons. In addition, it is possible that the average Mo to Re ratio of river bed materials does not well describe the rocks being weathered in these catchments, or that the river water isotopic and elemental composition varies with flow and our sampling has not captured a representative composition (King and Pett-Ridge, 2018).

Supplementary Tables

Table S-1 River bed material samples from the western Southern Alps, New Zealand (WSAlps), eastern Southern Alps, New Zealand (ESAlps), Mackenzie River basin, and Yukon River.

Location	Catchment	Collection date	Sample ID	Latitude (°)	Longitude (°)	$[Re]_{BM}$ (ppt)	$[OC]_{BM}$ %	$\delta^{98/95}$Mo (‰)*	2SD (‰)	Replicates	Mo (ppm)
Western Southern Alps											
WSAlps	Hokitika	14/09/2014	NZ14-19	42.95557	171.01666 E	87	0.11	-0.26	0.04	2	0.14
WSAlps	Wanganui	15/09/2014	NZ14-23	43.16322	170.62808 E	78	0.08	-0.38	0.00	2	0.18
WSAlps	Poerua	16/09/2014	NZ14-38	43.15672	170.50438 E	81	0.17	-0.27	0.03	3	0.21
WSAlps	Waitangitaona	16/09/2014	NZ14-35	43.28241	170.30812 E	252	0.18	-0.41	0.04	3	0.24
WSAlps	Callery	16/09/2014	NZ14-49	43.39675	170.18344 E	66	0.08	-0.30	0.05	2	0.23
WSAlps	Waiho	27/09/2014	NZ14-92	43.41808	170.18065 E	104	0.11	-0.31	0.01	4	0.29
WSAlps	Docherty Creek	27/09/2014	NZ14-90	43.38486	170.13333 E	112	0.21	-0.26	0.04	3	0.26
WSAlps			NZ14-90 duplicate					-0.26	0.06	3	0.25
WSAlps	Fox	18/09/2014	NZ14-64	43.49958	170.05521 E	241	0.13	-0.23	0.05	3	0.46
WSAlps	Fox	19/09/2014	NZ14-67	43.48704	170.02962 E	236	0.19	-0.18	0.05	4	0.65
WSAlps			NZ14-67 duplicate					-0.12	0.07	3	0.53
WSAlps	Cook	19/09/2014	NZ14-70	43.49912	169.9653 E	114	0.18	-0.24	0.05	3	0.32
WSAlps	Karangarua	19/09/2014	NZ14-72	43.57515	169.8051 E	76	0.17	-0.43	0.03	3	0.3
WSAlps	Haast	19/09/2014	NZ14-76	43.85398	169.05496 E	117	0.13	-0.43	0.04	3	0.22
Average WSAlps								*-0.31*	*0.05*		
ESAlps	Hooker Glacier	04/10/2014	NZ14-115	44.03936	169.37926 E	73	0.06	-0.34	0.00	2	0.16
ESAlps	Tasman River	04/10/2014	NZ14-119	43.70715	170.17097 E	82	0.06	-0.35	0.01	3	0.31
Mackenzie Basin	Peel, Fort McPherson	21/07/2009	CAN09-41	67.33189	134.86912	4356		0.19	0.02	5	3.44
Mackenzie Basin	Mackenzie, Tsiigehtchic	22/07/2009	CAN09-48	67.44935 N	133.74064 W	740		0.42	0.03	4	1.01
Mackenzie Basin	Mackenzie Delta, Middle Channel, Inuvik	08/09/2010	CAN10-27	68.44568 N	134.21349 W	1498		0.39	0.07	3	1.31
Mackenzie Basin	Ogilvie, Dempster	20/07/2013	CAN13-10	65.56789 N	138.17824 W	11354	0.9	0.53	0.06	3	7.98
Yukon	Yukon, Dawson City	21/07/2013	CAN13-23	64.04846 N	139.45628 W	1044	0.5	0.15	0.07	3	1.22
Average Mackenzie & Yukon								*0.34*	*0.16*		

*Reported as per Supplementary Equation S1 (NIST-SRM-3134 = 0 ‰). Re and OC data are from Horan *et al.* (2017) and Horan *et al.* (2019)

Table S-2 As per Table S-1, but for river suspended sediments.

Location	Catchment	Collection date	Sample	Latitude (°)	Longitude (°)	[Re] (ppt)	$\delta^{98/95}$Mo (‰)	2SD (‰)	Replicates	Mo (ppm)
WSAlps	Wanganui	16/09/2014	NZ14-40	43.15522 S	170.62608 E		-0.33	0.07	3	0.47
WSAlps	Poerua	16/09/2014	NZ14-37	43.15672 S	170.50438 E		-0.35	0.04	3	0.53
WSAlps			NZ14-37 duplicate			137	-0.35	0.06	3	0.63
WSAlps	Waitangitaona	16/09/2014	NZ14-34	43.28241 S	170.30812 E		-0.34	0.07	5	0.49
WSAlps	Waiho	16/09/2014	NZ14-47	43.41813 S	170.1806 E	116	-0.31	0.03	3	0.33
WSAlps			NZ14-47 duplicate				-0.25	0.08	3	0.32
WSAlps	Callery	16/09/2014	NZ14-48	43.39675 S	170.18344 E	103	-0.31	0.04	3	0.33
WSAlps			NZ14-48 duplicate			94	-0.39	0.07	3	0.31
WSAlps	Fox	18/09/2014	NZ14-66	43.48704 S	170.02962 E	332	-0.29	0.02	3	0.82
WSAlps			NZ14-66 duplicate			323	-0.28	0.03	3	0.79
WSAlps	Fox	27/09/2014	NZ14-86			112	-0.15	0.03	3	0.47
WSAlps			NZ14-86 duplicate				-0.24	0.07	3	0.34
WSAlps	Cook	19/09/2014	NZ14-69	43.49912 S	169.9653 E		-0.38	0.07	3	0.42
WSAlps	Karangarua	19/09/2014	NZ14-71	43.57515 S	169.8051 E		-0.25	0.02	3	0.56
WSAlps			NZ14-71 duplicate				-0.28	0.02	3	0.53
Mackenzie Basin	Peel River	26/07/2013	CAN13-68	67.33448 N	134.87762 W		0.21	0.01	3	3.06
Mackenzie Basin	Mackenzie River	26/07/2013	CAN13-74	67.45818 N	133.72734 W		0.39	0.01	3	2.06
Mackenzie Basin	Mackenzie River	24/07/2013	CAN13-58	68.41313 N	134.08893 W		0.35	0.03	3	2.30
Mackenzie Basin	Ogilvie River	22/07/2013	CAN13-34	65.36216 N	138.30226 W		0.49	0.02	3	3.23
Mackenzie Basin	Yukon River	21/07/2013	CAN13-17	64.04846 N	139.45628 W		0.15	0.04	3	2.46

Table S-3 River water samples from this study (as per Table S-1).

Location	Catchment	Collection date	Sample	Latitude	Longitude	pH	Temp.	Na^+	K^+	Mg^{2+}	Ca^{2+}	F^-	Cl^-	SO_4^{2-}	Total Alkalinity	HCO_3^-	$[Re]_{diss}$	$[Mo]_{diss}$	$\delta^{98/95}Mo$	2SD	n	fMo_{diss}	±	$\Delta^{98/95}Mo_{diss-BM}$	±
				(°)	(°)		(°C)	(µmol L^{-1})	(µmol L^{-1})	(µmol L^{-1})	(µmol L^{-1})	(µmol L^{-1})	(µmol L^{-1})	(µmol L^{-1})	(µmol L^{-1})	(µmol L^{-1})	(pmol L^{-1})	(nmol L^{-1})	(‰)	(‰)				(‰)	
WSAlps	Hokitika	14/09/2014	NZ14-18	42.95557 S	171.01666 E	8.36	8.4	57.83	25.38	13.99	186.5	1.58	31.31	32.74	506	500	1.7	5.84	0.11	0.03	5	0.72	0.16	0.42	0.06
WSAlps	Wanganui	16/09/2014	NZ14-40	43.15522 S	170.62608 E	8.14	6.4	53.91	19.49	7	130.25	1.05	59.52	41.47	423	420	1.69	6.36	0.01	0.04	2	0.8	0.17	0.31	0.06
WSAlps	Poerua	16/09/2014	NZ14-37	43.15672 S	170.50438 E	7.74	8	71.74	31.79	13.58	139.5	0.53	85.19	31.49	306	305	1.47	3.73	0.08	0.01	2	0.53	0.12	0.39	0.05
WSAlps	Waitangitaona	16/09/2014	NZ14-34	43.28241 S	170.30812 E	8.2	7	58.26	30	14.81	129.75	1.05	50.21	31.81	327	324	1.33	2.77	0.13	0.02	2	0.44	0.09	0.43	0.05
WSAlps	Waiho	16/09/2014	NZ14-47	43.41813 S	170.18060 E	8.48	3.8	53.48	88.97	52.26	493.5	1.05	26.8	192.08	1111	1095	7.56	14.45	0.14	0.01	2	0.4	0.09	0.45	0.05
WSAlps	Waiho	02/10/2014	NZ14-107	43.61212 S	169.85655 E	8.34	4.1	57.83	88.72	55.56	491.5	1.05	21.16	198.63	1109	1097	6.13	15.34	0.15	0.02	3	0.53	0.11	0.46	0.05
WSAlps	Callery	16/09/2014	NZ14-48	43.39675 S	170.18344 E	8.43	5.4	74.78	35.9	22.22	398	1.05	26.23	94.79	894	882	2.55	13.7	0.00	0.01	2	1.13	0.24	0.3	0.05
WSAlps	Callery	02/10/2014	NZ14-108	43.39725 S	170.18408 E	8.42	6.8	58.7	29.74	17.28	317.75	1.05	24.82	115.06	1032	1019	3.09	15.22	0.04	0.03	3	1.04	0.22	0.35	0.06
WSAlps	Fox	18/09/2014	NZ14-66	43.48704 S	170.02962 E	8.52	3.3	112.61	144.1	92.18	722.75	1.58	32.16	274.09	1620	1595	11.55	18.33	0.32	0.03	5	0.33	0.07	0.62	0.06
WSAlps	Fox	27/09/2014	NZ14-86	43.48704 S	170.02962 E	8.67	1.1	50.87	111.79	57.2	463	0.53	19.18	178.98	1058	1035	6.78	13.73	0.17	0.12	2	0.43	0.09	0.48	0.12
WSAlps	Cook	19/09/2014	NZ14-69	43.49912 S	169.9653 E	8.48	6.4	51.74	28.46	16.87	174.25	0.53	47.95	41.78	438	431	1.85	6.16	0.04	0.01	2	0.7	0.15	0.35	0.05
WSAlps	Karangarua	19/09/2014	NZ14-71	43.57515 S	169.8051 E	8.18	7.3	45.65	19.49	10.29	91	0	41.75	16.84	224	223	0.84	2.13	0.06	0.01	2	0.54	0.12	0.37	0.05
WSAlps	Haast	19/09/2014	NZ14-75	43.85398 S	169.05496 E	8.09	8.6	59.57	21.54	20.99	220.5	1.05	37.8	34.3	606	602	2.01	4.25	0.28	0.03	2	0.44	0.10	0.59	0.06
ESAlps	Hooker	04/10/2014	NZ14-116	43.69284 S	170.09869 E	8.39	2.1	30.87	11.28	16.46	169.25	0.53	8.74	74.21	525	518	0.91	7.33	-0.16	0.05	3				
ESAlps	Hooker	04/10/2014	NZ14-117	43.69269 S	170.09903 E	8.29	4.1	48.26	15.64	28.81	279.75	0.53	11	72.03	655	649	1.24		0.03	0.08	3				
ESAlps	Tasman	04/10/2014	NZ14-118	43.70715 S	170.17097 E	8.43	3.2	67.39	17.44	15.23	240.75	0.53	7.33	82.32	547	540	1.05	12.1	-0.19	0.04	3				
Mackenzie Basin	Peel, Fort McPherson	26/07/2013	CAN13-81	67.33448 N	134.87762 W			159.04	12.68	690.4	1162.18		36.51	797.14		2350	19.31	12.98	1.22	0.04	2	0.44	0.10	1.03	0.05
Mackenzie Basin	Mackenzie, Tsiigehtchic	26/07/2013	CAN13-82	67.45818 N	133.72734 W			133.59	19.23	398.33	868.36		188.97	451.03		1918	17.87	11.07	1.13	0.04	2	0.23	0.05	0.71	0.05
Mackenzie Basin	Mackenzie Delta, Inuvik	24/07/2013	CAN13-65	68.41313 N	134.08893	8.04	16.9	123.64	18.29	384.71	842.04		163.42	454.22		1973	19.57	12.5	0.96	0.01	2	0.38	0.08	0.57	0.07
Mackenzie Basin	Ogilvie River, Dempster bridge	20/07/2013	CAN13-12	65.36131 N	138.17824 W	8.26	12.9	521.85	11.32	691.58	1249.46		73.13	1147.58		2703	27.92	18.94	1.53	0.04	2	0.5	0.11	1.01	0.07
Yukon	Yukon, Dawson City	21/07/2013	CAN13-22	64.04846 N	139.45628 W	8.22	15.5	117.45	45.39	350.49	748.38		15.71	353.91		1713	16.9	17.68	0.73	0.02	2	0.46	0.10	0.58	0.07
Iceland	Skaftá	19/08/2014	Skaftá-1	63.79233 N	18.03727 W	8.02		299.51	14.36	115.23	223.75	5.26	137.66	88.56	630		4.22	1.7	0.37	0.03	1	0.39	0.08	0.52	0.06
Iceland	Skaftá	19/08/2014	Skaftá-2	63.79277 N	18.49555 W	8.47		258.17	12.31	87.24	176.75	4.74	77.86	72.97	676		3.26	1.78	0.35	0.03	1	0.52	0.11	0.5	0.06
Iceland	Skaftá	19/08/2014	Skaftá-3G	63.91005 N	18.59857 W	7.31		265.37	9.49	108.23	228	3.68	47.39	77.95			3.49	1.55	0.39	0.03	1	0.43	0.09	0.54	0.06
Iceland	Skaftá	19/08/2014	Skaftá-4	64.07949 N	18.40699 W	7.67		320.26	12.82	141.56	312.5	4.74	48.8	103.21			3.8	1.54	0.47	0.03	1	0.39	0.08	0.62	0.06
Iceland	Skaftá tributary	19/08/2014	Skaftá- 3NG	63.91005 N	18.59857 W	5.91		398.41	10.26	23.46	59.25	4.21	77.57	29.31			4.99	3.13	0.26	0.03	1	0.6	0.13	0.41	0.06

Table S-4 Soil litter and weathered colluvium from the western Southern Alps.

Location	Sample type	Sample ID	Lat. (°S)	Long. (°E)	[OC] %	Re (ppt)	$\delta^{98/95}$Mo	2SD	Replicates	[Mo] (ppm)
WSAlps	Weathered colluvium	NZ14-54	43.40796	170.16727	1.26	36.1	-0.32	0.06	3	0.29
WSAlps	Weathered colluvium	NZ14-55	43.40602	170.16171	1.54	31.4	-0.32	0.05	3	0.23
WSAlps	Weathered colluvium	NZ14-56	43.40602	170.16171	0.88	23.7	-0.90	0.02	2	0.24
WSAlps		NZ14-56 duplicate					-0.81	0.05	3	0.25
WSAlps	Weathered colluvium	NZ14-59	43.40596	170.16115	0.96	24.2	-0.54	0.04	2	0.34
WSAlps		NZ14-59 duplicate					-0.42	0.10	3	0.34
WSAlps	Surface soil	NZ14-57	43.40596	170.16115	4.16	24.7	-0.33	0.07	2	0.25
WSAlps	Surface soil	NZ14-58	43.40596	170.16115	5.97	21.3	-0.09	0.01	3	0.41
WSAlps		NZ14-58 duplicate					-0.15	0.03	3	0.42
WSAlps		NZ14-60	43.40596	170.16115	13.24	52	-0.14	0.02	3	0.36
WSAlps	Surface soil	NZ14-61	43.40909	170.16335	10.48	27	-0.36	0.05	3	0.27
WSAlps		NZ14-61 duplicate					-0.24	0.07	3	0.28
WSAlps	Surface soil	NZ14-62	43.41448	170.15887	7.44	21.7	-0.21	0.06	3	0.24
WSAlps	Local river bed material	NZ14-90	43.38486	170.13333	0.21	111	-0.26	0.04	3	0.26
WSAlps		NZ14-90 duplicate					-0.26	0.06	3	0.25

Table S-5 BHVO-1 and IAPSO measurements.

Standard	Sample No.	Replicates	$\delta^{98/95}$Mo (‰)	2SE analytical error (‰)	Average $\delta^{98/95}$Mo (‰)	2SD (‰)	[Mo] (ppm)*	Average Mo (ppm)	2SD (ppm)
BHVO-1	1	1	-0.206	0.019			1.00		
	2	3	-0.156	0.022	-0.181	0.054	1.00	1.00	0.00
			-0.177	0.016			1.00		
			-0.210	0.016			0.99		
	3	3	-0.200	0.018	-0.198	0.011	0.97	0.97	0.00
			-0.192	0.019			0.97		
			-0.202	0.015			0.96		
	4	3	-0.198	0.020	-0.212	0.043	1.00	1.00	0.00
			-0.237	0.015			0.99		
			-0.201	0.016			1.00		
	5	3	-0.200	0.023	-0.201	0.010	1.03	1.03	0.00
			-0.206	0.027			1.03		
			-0.196	0.020			1.03		
	6	4	-0.173	0.018	-0.161	0.027	1.03	1.03	0.00
			-0.157	0.017			1.03		
			-0.143	0.016			1.03		
			-0.170	0.014			1.03		
	7	4	-0.192	0.022	-0.192	0.031	0.97	0.97	0.00
			-0.171	0.016			0.97		
			-0.209	0.015			0.97		
			-0.194	0.018			0.97		
	All samples				-0.190	0.044		1.00	0.05
IAPSO	1	2	2.098	0.019	2.099	0.001	11.16	11.16	
			2.099	0.015			11.16		
	2	2	2.057	0.017	2.046	0.033	11.00	11.00	
			2.034	0.018			11.00		
	3	1	2.066	0.021			10.10		
	All samples				2.071	0.056	10.89		0.45

* 2SE analytical errors all <0.00 ppm

Table S-6 Compilation of river, stream and groundwater measurements, adapted from King and Pett Ridge (2018).

River	Source	[Mo] nmol/L	Published δ^{98}Mo (‰)	Primary Standard*	Correction to NIST-3134 (‰)**	Correction to published value required relative to NIST-3134 (‰)	δ^{98}Mo (NIST-3134 = 0) (‰)
Itchen	Archer and Vance, 2008	4.84	1.14	BIG-Mo	-0.26	-0.26	0.88
Kalix	Archer and Vance, 2008	7.74	1.00	BIG-Mo	-0.26	-0.26	0.74
Kalix	Archer and Vance, 2008	5.55	1.20	BIG-Mo	-0.26	-0.26	0.94
Kalix	Archer and Vance, 2008	5.03	1.05	BIG-Mo	-0.26	-0.26	0.79
Kalix	Archer and Vance, 2008	4.94	0.98	BIG-Mo	-0.26	-0.26	0.72
Kalix	Archer and Vance, 2008	4.91	1.11	BIG-Mo	-0.26	-0.26	0.85
Kalix	Archer and Vance, 2008	4.88	1.00	BIG-Mo	-0.26	-0.26	0.74
Nile	Archer and Vance, 2008	7.33	0.17	BIG-Mo	-0.26	-0.26	-0.09
Nile	Archer and Vance, 2008	4.45	0.78	BIG-Mo	-0.26	-0.26	0.52
Nile	Archer and Vance, 2008	11.11	0.38	BIG-Mo	-0.26	-0.26	0.12
Nile	Archer and Vance, 2008	18.11	0.44	BIG-Mo	-0.26	-0.26	0.18
Nile	Archer and Vance, 2008	13.31	0.48	BIG-Mo	-0.26	-0.26	0.22
Nile	Archer and Vance, 2008	4.96	1.20	BIG-Mo	-0.26	-0.26	0.94
Nile	Archer and Vance, 2008	3.59	1.40	BIG-Mo	-0.26	-0.26	1.14
Nile	Archer and Vance, 2008	7.99	0.15	BIG-Mo	-0.26	-0.26	-0.11
Nile	Archer and Vance, 2008	7.07	0.48	BIG-Mo	-0.26	-0.26	0.22
Volga	Archer and Vance, 2008	6.65	1.19	BIG-Mo	-0.26	-0.26	0.93
Chang Jiang	Archer and Vance, 2008	16.71	0.95	BIG-Mo	-0.26	-0.26	0.69
Chang Jiang	Archer and Vance, 2008	16.81	0.65	BIG-Mo	-0.26	-0.26	0.39
Chang Jiang	Archer and Vance, 2008	17.71	0.89	BIG-Mo	-0.26	-0.26	0.63
Chang Jiang	Archer and Vance, 2008	17.11	0.83	BIG-Mo	-0.26	-0.26	0.57
Chang Jiang	Archer and Vance, 2008	15.91	0.90	BIG-Mo	-0.26	-0.26	0.64
Ottawa	Archer and Vance, 2008	2.17	2.25	BIG-Mo	-0.26	-0.26	1.99
Ottawa	Archer and Vance, 2008	2	2.40	BIG-Mo	-0.26	-0.26	2.14
Clear Creek	Archer and Vance, 2008	507.32	0.24	BIG-Mo	-0.26	-0.26	-0.02
Clear Creek	Archer and Vance, 2008	508.32	0.23	BIG-Mo	-0.26	-0.26	-0.03
Clear Creek	Archer and Vance, 2008	511.32	0.24	BIG-Mo	-0.26	-0.26	-0.02
Clear Creek	Archer and Vance, 2008	507.32	0.23	BIG-Mo	-0.26	-0.26	-0.03
Brahamaputra	Archer and Vance, 2008	8.98	0.74	BIG-Mo	-0.26	-0.26	0.48
Amazon	Archer and Vance, 2008	4.34	0.57	BIG-Mo	-0.26	-0.26	0.31
Amazon	Archer and Vance, 2008	4.3	0.63	BIG-Mo	-0.26	-0.26	0.37

River	Source	[Mo] nmol/L	Published δ^{98}Mo (‰)	Primary Standard*	Correction to NIST-3134 (‰)**	Correction to published value required relative to NIST-3134 (‰)	δ^{98}Mo (NIST-3134 = 0) (‰)
SE Iceland	Pearce *et al.*, 2010	2.59	-0.13	OU-Mo	-0.37	-0.37	-0.50
SE Iceland	Pearce *et al.*, 2010	7.66	1.51	OU-Mo	-0.37	-0.37	1.14
SE Iceland	Pearce *et al.*, 2010	2.94	0.07	OU-Mo	-0.37	-0.37	-0.30
SE Iceland	Pearce *et al.*, 2010	1.3	-0.01	OU-Mo	-0.37	-0.37	-0.38
SE Iceland	Pearce *et al.*, 2010	1.56	0.49	OU-Mo	-0.37	-0.37	0.12
W Iceland	Pearce *et al.*, 2010	2.82	0.95	OU-Mo	-0.37	-0.37	0.58
W Iceland	Pearce *et al.*, 2010	2.82	0.95	OU-Mo	-0.37	-0.37	0.58
W Iceland	Pearce *et al.*, 2010	3.15	0.90	OU-Mo	-0.37	-0.37	0.53
W Iceland	Pearce *et al.*, 2010	3.95	0.96	OU-Mo	-0.37	-0.37	0.59
W Iceland	Pearce *et al.*, 2010	3.17	1.00	OU-Mo	-0.37	-0.37	0.63
W Iceland	Pearce *et al.*, 2010	2.65	0.60	OU-Mo	-0.37	-0.37	0.23
W Iceland	Pearce *et al.*, 2010	8.91	0.44	OU-Mo	-0.37	-0.37	0.07
W Iceland	Pearce *et al.*, 2010	3.7	0.71	OU-Mo	-0.37	-0.37	0.34
W Iceland	Pearce *et al.*, 2010	1.86	0.39	OU-Mo	-0.37	-0.37	0.02
W Iceland	Pearce *et al.*, 2010	3.05	0.63	OU-Mo	-0.37	-0.37	0.26
W Iceland	Pearce *et al.*, 2010	0.8	1.77	OU-Mo	-0.37	-0.37	1.40
W Iceland	Pearce *et al.*, 2010	1.74	1.10	OU-Mo	-0.37	-0.37	0.73
Chang Jiang	Neubert *et al.*, 2011	9.01	1.22	Bern-Mo	-0.27	-0.27	0.95
Chang Jiang	Neubert *et al.*, 2011	13.01	1.11	Bern-Mo	-0.27	-0.27	0.84
Entlebuch	Neubert *et al.*, 2011	1.79	0.46	Bern-Mo	-0.27	-0.27	0.19
Entlebuch	Neubert *et al.*, 2011	1.11	0.36	Bern-Mo	-0.27	-0.27	0.09
Entlebuch	Neubert *et al.*, 2011	1.65	0.35	Bern-Mo	-0.27	-0.27	0.08
Entlebuch	Neubert *et al.*, 2011	0.9	0.16	Bern-Mo	-0.27	-0.27	-0.11
Entlebuch	Neubert *et al.*, 2011	0.71	0.14	Bern-Mo	-0.27	-0.27	-0.13
Entlebuch	Neubert *et al.*, 2011	0.53	0.27	Bern-Mo	-0.27	-0.27	0.00
Entlebuch	Neubert *et al.*, 2011	2.95	1.25	Bern-Mo	-0.27	-0.27	0.98
Entlebuch	Neubert *et al.*, 2011	2.45	1.50	Bern-Mo	-0.27	-0.27	1.23
Entlebuch	Neubert *et al.*, 2011	2.71	1.29	Bern-Mo	-0.27	-0.27	1.02
Entlebuch	Neubert *et al.*, 2011	2.69	1.60	Bern-Mo	-0.27	-0.27	1.33
Entlebuch	Neubert *et al.*, 2011	1.97	1.09	Bern-Mo	-0.27	-0.27	0.82
Entlebuch	Neubert *et al.*, 2011	2.34	1.01	Bern-Mo	-0.27	-0.27	0.74
Entlebuch	Neubert *et al.*, 2011	2.49	1.21	Bern-Mo	-0.27	-0.27	0.94
Aare	Neubert *et al.*, 2011	5.09	1.22	Bern-Mo	-0.27	-0.27	0.95
Aare	Neubert *et al.*, 2011	5.69	1.13	Bern-Mo	-0.27	-0.27	0.86

River	Source	[Mo] nmol/L	Published δ^{98}Mo (‰)	Primary Standard*	Correction to NIST-3134 (‰)**	Correction to published value required relative to NIST-3134 (‰)	δ^{98}Mo (NIST-3134 = 0) (‰)
Aare	Neubert *et al.*, 2011	5.82	1.34	Bern-Mo	-0.27	-0.27	1.07
Aare	Neubert *et al.*, 2011	6.94	1.04	Bern-Mo	-0.27	-0.27	0.77
Aare	Neubert *et al.*, 2011	7.18	1.05	Bern-Mo	-0.27	-0.27	0.78
Aare	Neubert *et al.*, 2011	9.13	0.90	Bern-Mo	-0.27	-0.27	0.63
Aare	Neubert *et al.*, 2011	2.08	1.90	Bern-Mo	-0.27	-0.27	1.63
Sikkim	Neubert *et al.*, 2011	139.09	0.59	Bern-Mo	-0.27	-0.27	0.32
Sikkim	Neubert *et al.*, 2011	43.03	0.56	Bern-Mo	-0.27	-0.27	0.29
Sikkim	Neubert *et al.*, 2011	90.06	0.57	Bern-Mo	-0.27	-0.27	0.30
Sikkim	Neubert *et al.*, 2011	44.03	0.66	Bern-Mo	-0.27	-0.27	0.39
Susquehanna	Scheiderich *et al.*, 2010	2.81	1.02	Mary-Mo	-0.16	-0.16	0.86
Malaval	Voegelin *et al.*, 2012	8.44	1.13	Bern-Mo	-0.27	-0.27	0.86
Malaval	Voegelin *et al.*, 2012	3.13	0.72	Bern-Mo	-0.27	-0.27	0.45
Sejallieres	Voegelin *et al.*, 2012	2.08	1.07	Bern-Mo	-0.27	-0.27	0.80
Sejallieres	Voegelin *et al.*, 2012	1.77	1.02	Bern-Mo	-0.27	-0.27	0.75
Malaval	Voegelin *et al.*, 2012	0.21	0.83	Bern-Mo	-0.27	-0.27	0.56
Malaval	Voegelin *et al.*, 2012	0.42	0.67	Bern-Mo	-0.27	-0.27	0.40
Malaval	Voegelin *et al.*, 2012	1.56	0.73	Bern-Mo	-0.27	-0.27	0.46
Malaval	Voegelin *et al.*, 2012	1.25	0.65	Bern-Mo	-0.27	-0.27	0.38
Malaval	Voegelin *et al.*, 2012	1.25	0.55	Bern-Mo	-0.27	-0.27	0.28
Malaval	Voegelin *et al.*, 2012	1.56	0.58	Bern-Mo	-0.27	-0.27	0.31
Malaval	Voegelin *et al.*, 2012	0.73	0.91	Bern-Mo	-0.27	-0.27	0.64
Malaval	Voegelin *et al.*, 2012	1.46	0.67	Bern-Mo	-0.27	-0.27	0.40
Narmada	Rahaman *et al.*, 2014	4.3	0.40	Bern-Mo	-0.27	-0.27	0.13
Tapi	Rahaman *et al.*, 2014	6.1	1.10	Bern-Mo	-0.27	-0.27	0.83
Xijang	Wang *et al.*, 2015	9.32	1.09	NIST-3134	0	0	1.09
Xijang	Wang *et al.*, 2015	10.46	1.04	NIST-3134	0	0	1.04
Xijang	Wang *et al.*, 2015	7.95	1.18	NIST-3134	0	0	1.18
Xijang	Wang *et al.*, 2015	4.32	1.30	NIST-3134	0	0	1.30
Xijang	Wang *et al.*, 2015	5.59	1.31	NIST-3134	0	0	1.31
Xijang	Wang *et al.*, 2015	5.53	1.25	NIST-3134	0	0	1.25
Xijang	Wang *et al.*, 2015	5.28	1.24	NIST-3134	0	0	1.24
Xijang	Wang *et al.*, 2015	7.79	1.18	NIST-3134	0	0	1.18
Xijang	Wang *et al.*, 2015	7.55	1.17	NIST-3134	0	0	1.17
Xijang	Wang *et al.*, 2015	6.8	1.24	NIST-3134	0	0	1.24

River	Source	[Mo] nmol/L	Published δ^{98}Mo (‰)	Primary Standard*	Correction to NIST-3134 (‰)**	Correction to published value required relative to NIST-3134 (‰)	δ^{98}Mo (NIST-3134 = 0) (‰)
Xijang	Wang *et al.*, 2015	7.37	1.27	NIST-3134	0	0	1.27
Xijang	Wang *et al.*, 2015	7.49	1.14	NIST-3134	0	0	1.14
Xijang	Wang *et al.*, 2015	7.33	1.14	NIST-3134	0	0	1.14
Xijang	Wang *et al.*, 2015	7.36	1.16	NIST-3134	0	0	1.16
Xijang	Wang *et al.*, 2015	7.5	1.24	NIST-3134	0	0	1.24
Xijang	Wang *et al.*, 2015	7.3	1.17	NIST-3134	0	0	1.17
Xijang	Wang *et al.*, 2015	6.98	1.22	NIST-3134	0	0	1.22
Huanghe	Wang *et al.*, 2015	97.96	0.17	NIST-3134	0	0	0.17
Huanghe	Wang *et al.*, 2015	88.16	0.25	NIST-3134	0	0	0.25
Huanghe	Wang *et al.*, 2015	85.45	0.28	NIST-3134	0	0	0.28
Huanghe	Wang *et al.*, 2015	89.46	0.30	NIST-3134	0	0	0.30
Huanghe	Wang *et al.*, 2015	79.45	0.38	NIST-3134	0	0	0.38
Huanghe	Wang *et al.*, 2015	112.07	0.24	NIST-3134	0	0	0.24
Huanghe	Wang *et al.*, 2015	11.01	0.37	NIST-3134	0	0	0.37
Huanghe	Wang *et al.*, 2015	95.66	0.36	NIST-3134	0	0	0.36
Huanghe	Wang *et al.*, 2015	89.16	0.35	NIST-3134	0	0	0.35
Huanghe	Wang *et al.*, 2015	92.26	0.22	NIST-3134	0	0	0.22
Huanghe	Wang *et al.*, 2015	117.07	0.28	NIST-3134	0	0	0.28
Huanghe	Wang *et al.*, 2015	123.08	0.09	NIST-3134	0	0	0.09
Huanghe	Wang *et al.*, 2015	110.07	0.12	NIST-3134	0	0	0.12
Huanghe	Wang *et al.*, 2015	101.06	0.15	NIST-3134	0	0	0.15
Huanghe	Wang *et al.*, 2015	82.95	0.29	NIST-3134	0	0	0.29
Eel River, South Fork	King and Pett Ridge, 2018	1.3	1.15	NIST-3134	0	-0.25	0.90
Johnston Draw	King and Pett Ridge, 2018	1.91	1.02	NIST-3134	0	-0.25	0.77
Reynolds Mountain	King and Pett Ridge, 2018	0.77	1.08	NIST-3134	0	-0.25	0.83
Marshall Gulch	King and Pett Ridge, 2018	81.11	0.50	NIST-3134	0	-0.25	0.25
Rose Hill	King and Pett Ridge, 2018	0.15	1.03	NIST-3134	0	-0.25	0.78
Gordon Gulch	King and Pett Ridge, 2018	9.04	1.36	NIST-3134	0	-0.25	1.11
Mamayes	King and Pett Ridge, 2018	0.61	1.44	NIST-3134	0	-0.25	1.19
Icacos	King and Pett Ridge, 2018	0.29	0.61	NIST-3134	0	-0.25	0.36
Guaba	King and Pett Ridge, 2018	0.38	1.24	NIST-3134	0	-0.25	0.99
Providence Creek	King and Pett Ridge, 2018	0.7	1.16	NIST-3134	0	-0.25	0.91
Weir 4, Calhoun	King and Pett Ridge, 2018	0.62	1.35	NIST-3134	0	-0.25	1.10
Holcomb	King and Pett Ridge, 2018	2.01	0.92	NIST-3134	0	-0.25	0.67

River	Source	[Mo] nmol/L	Published δ^{98}Mo (‰)	Primary Standard*	Correction to NIST-3134 (‰)**	Correction to published value required relative to NIST-3134 (‰)	δ^{98}Mo (NIST-3134 = 0) (‰)
Honoli'i	King and Pett Ridge, 2018	0.1	-0.28	NIST-3134	0	-0.25	-0.53
MCG-5	King and Pett Ridge, 2018	0.17	-0.22	NIST-3134	0	-0.25	-0.47
Kolekole	King and Pett Ridge, 2018	4.68	0.04	NIST-3134	0	-0.25	-0.21
Makahiloa	King and Pett Ridge, 2018	0.15	0.24	NIST-3134	0	-0.25	-0.01
Waipi'o	King and Pett Ridge, 2018	7.49	0.24	NIST-3134	0	-0.25	-0.01
PW4	King and Pett Ridge, 2018	21.61	0.25	NIST-3134	0	-0.25	0.00
WP87	King and Pett Ridge, 2018	1.18	0.32	NIST-3134	0	-0.25	0.07
Ke'ei	King and Pett Ridge, 2018	11.43	0.34	NIST-3134	0	-0.25	0.09
PW7	King and Pett Ridge, 2018	40.82	0.36	NIST-3134	0	-0.25	0.11
WR@dam	King and Pett Ridge, 2018	0.37	0.36	NIST-3134	0	-0.25	0.11
Kalaoa	King and Pett Ridge, 2018	16.92	0.44	NIST-3134	0	-0.25	0.19
Honokōhau	King and Pett Ridge, 2018	164.11	0.44	NIST-3134	0	-0.25	0.19
PW1	King and Pett Ridge, 2018	22.23	0.45	NIST-3134	0	-0.25	0.20
Pololu-1	King and Pett Ridge, 2018	1.54	0.50	NIST-3134	0	-0.25	0.25
Puu Lani	King and Pett Ridge, 2018	37.41	0.51	NIST-3134	0	-0.25	0.26
WE@powerhouse	King and Pett Ridge, 2018	0.72	0.54	NIST-3134	0	-0.25	0.29
WR@Po'o Koeha	King and Pett Ridge, 2018	0.54	0.56	NIST-3134	0	-0.25	0.31
Manoloa	King and Pett Ridge, 2018	0.14	0.61	NIST-3134	0	-0.25	0.36
MCG-3	King and Pett Ridge, 2018	0.13	0.74	NIST-3134	0	-0.25	0.49
Kapue	King and Pett Ridge, 2018	0.14	0.88	NIST-3134	0	-0.25	0.63
WR @ Ford	King and Pett Ridge, 2018	0.5	0.90	NIST-3134	0	-0.25	0.65
Koke'e Up	King and Pett Ridge, 2018	0.07	1.12	NIST-3134	0	-0.25	0.87
AB-2	Neely *et al.*, 2018	0.33	0.29	NIST-3134	0	-0.25	0.04
LUD-4	Neely *et al.*, 2018	1.52	1.12	NIST-3134	0	-0.25	0.87
LUD-2	Neely *et al.*, 2018	0.57	0.39	NIST-3134	0	-0.25	0.14
LUD-3	Neely *et al.*, 2018	0.59	0.39	NIST-3134	0	-0.25	0.14
Garoslind	Neely *et al.*, 2018	0.65	0.47	NIST-3134	0	-0.25	0.22
Hverdjallasgja	Neely *et al.*, 2018	0.71	0.38	NIST-3134	0	-0.25	0.13
Vagafloi	Neely *et al.*, 2018	0.81	0.33	NIST-3134	0	-0.25	0.08
Peistareykirvatnsbol	Neely *et al.*, 2018	0.18	0.68	NIST-3134	0	-0.25	0.43
Krossdalur	Neely *et al.*, 2018	0.18	0.00	NIST-3134	0	-0.25	-0.25
Fjoll-lind	Neely *et al.*, 2018	0.21	-0.08	NIST-3134	0	-0.25	-0.33
Fjoll-vatnsbol	Neely *et al.*, 2018	0.1	0.17	NIST-3134	0	-0.25	-0.08
Lon	Neely *et al.*, 2018	0.26	0.06	NIST-3134	0	-0.25	-0.19

River	Source	[Mo] nmol/L	Published δ^{98}Mo (‰)	Primary Standard*	Correction to NIST-3134 (‰)**	Correction to published value required relative to NIST-3134 (‰)	δ^{98}Mo (NIST-3134 = 0) (‰)
PR-8	Neely *et al.*, 2018	0.1	-0.15	NIST-3134	0	-0.25	-0.40
PR-16	Neely *et al.*, 2018	0.19	-0.04	NIST-3134	0	-0.25	-0.29
Hokitika	This study	5.84	0.11	NIST-3134	0	0	0.11
Wanganui	This study	6.36	0.01	NIST-3134	0	0	0.01
Poerua	This study	3.73	0.08	NIST-3134	0	0	0.08
Waitangitaona	This study	2.77	0.13	NIST-3134	0	0	0.13
Waiho	This study	14.45	0.14	NIST-3134	0	0	0.14
Waiho	This study	15.34	0.15	NIST-3134	0	0	0.15
Callery	This study	13.7	0.00	NIST-3134	0	0	0.00
Callery	This study	15.22	0.04	NIST-3134	0	0	0.04
Fox	This study	18.33	0.32	NIST-3134	0	0	0.32
Fox	This study	13.73	0.17	NIST-3134	0	0	0.17
Cook	This study	6.16	0.04	NIST-3134	0	0	0.04
Karangarua	This study	2.13	0.06	NIST-3134	0	0	0.06
Haast	This study	4.25	0.28	NIST-3134	0	0	0.28
Hooker	This study	7.33	-0.16	NIST-3134	0	0	-0.16
Hooker	This study		0.03	NIST-3134	0	0	0.03
Tasman	This study	12.1	-0.19	NIST-3134	0	0	-0.19
Peel, Fort McPherson	This study	12.98	1.22	NIST-3134	0	0	1.22
Mackenzie, Tsiigehtchic	This study	11.07	1.13	NIST-3134	0	0	1.13
Mackenzie Delta, Inuvik	This study	12.5	0.96	NIST-3134	0	0	0.96
Ogilvie River, Dempster bridge	This study	18.94	1.53	NIST-3134	0	0	1.53
Yukon, Dawson City	This study	17.68	0.73	NIST-3134	0	0	0.73
Skaftá	This study	1.70	0.37	NIST-3134	0	0	0.37
Skaftá	This study	1.78	0.35	NIST-3134	0	0	0.35
Skaftá	This study	1.55	0.39	NIST-3134	0	0	0.39
Skaftá	This study	1.54	0.47	NIST-3134	0	0	0.47
Skaftá tributary	This study	3.13	0.26	NIST-3134	0	0	0.26

* Notation following Goldberg *et al*. (2013). **Shift in δ^{98}Mo values based on average of standard composition measured relative to NIST-SRM-3134 from Goldberg *et al*. (2013).

Supplementary Figures

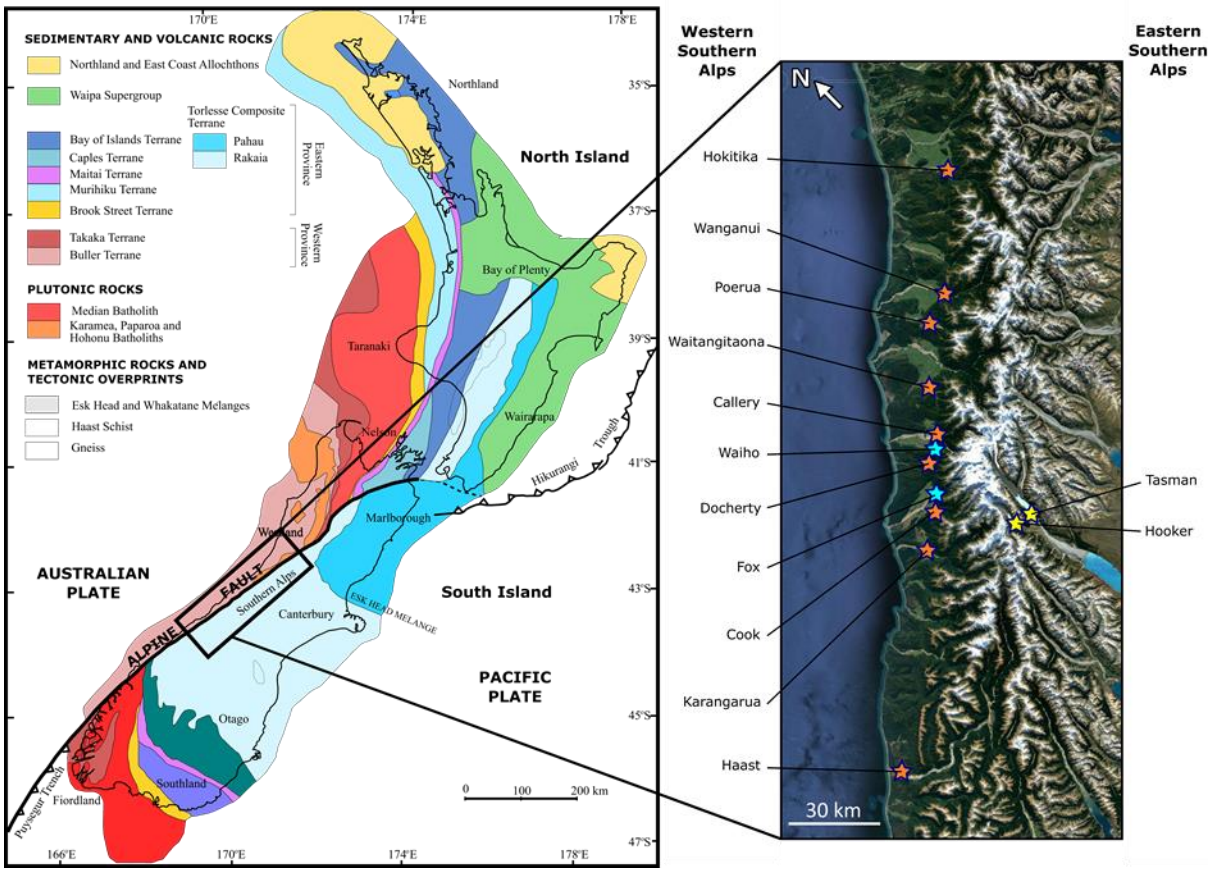

Figure S-1 Geological map of New Zealand based on Mortimer *et al*. (2004). Inset indicates catchments sampled in the western and eastern Southern Alps. The red and blue stars indicate sampled catchments with <45 % and >45 % glacial coverage, respectively, in the western Southern Alps. The yellow stars indicate sampled catchments in the eastern Southern Alps.

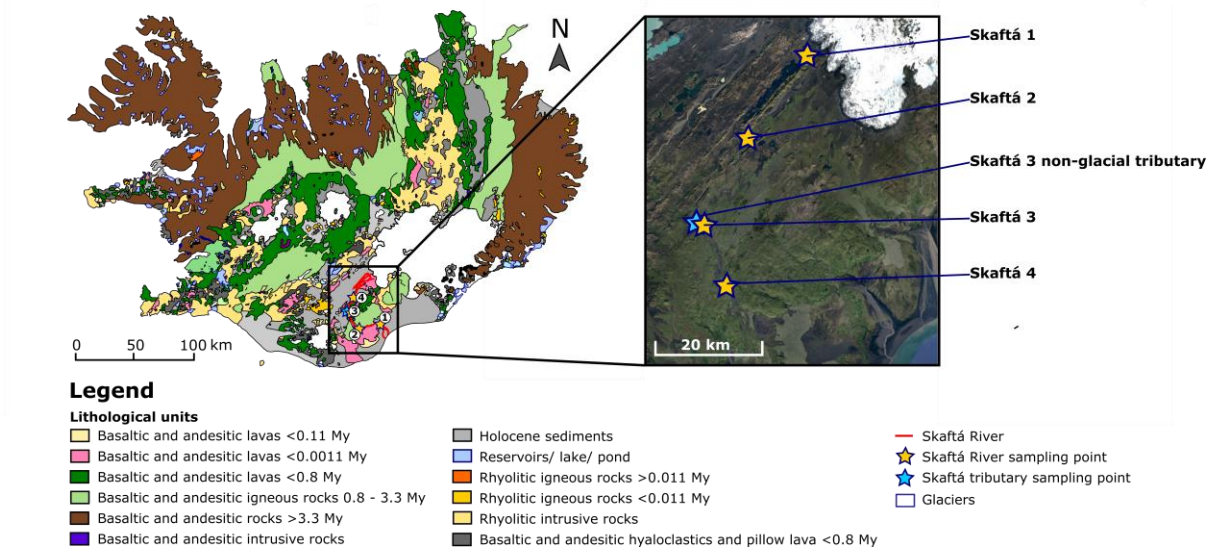

Figure S-2 Geological map of Iceland with inset showing sampling localities along the Skaftá River and its tributary to the west. Geological map is adapted from Oskarsdottir *et al*. (2011).

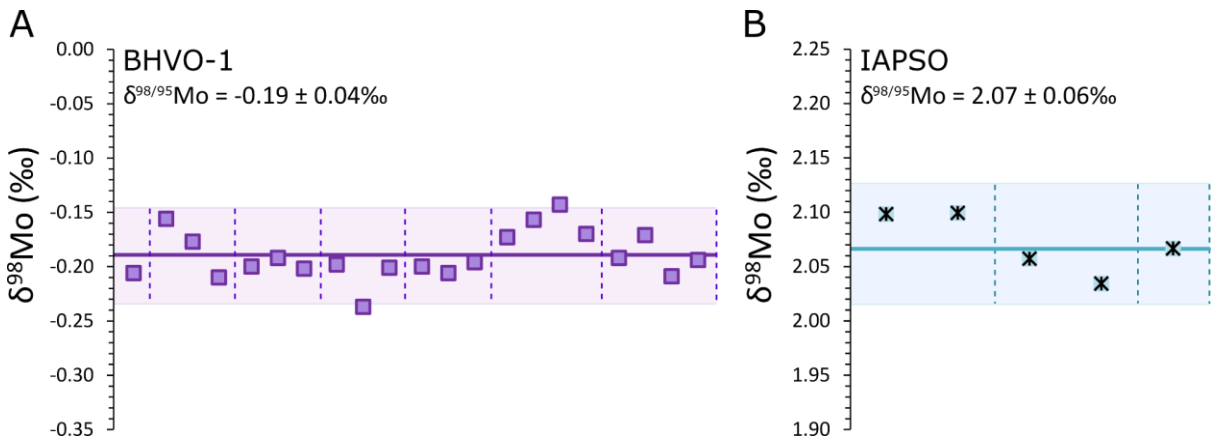

Figure S-3 Long-term reproducibility of standards used in Mo isotope analyses. **A.** BHVO-1. Thick purple line shows the mean value. **B.** IAPSO seawater salinity reference material. Thick blue line shows the mean value. The ±2 SD errors on the long-term mean replicate values are indicated within the shaded bands. The ±2 SE analytical error on an individual measurement is smaller than the point size. Separate analytical sessions are marked with dashed vertical lines. Data can be found in Table S-5.

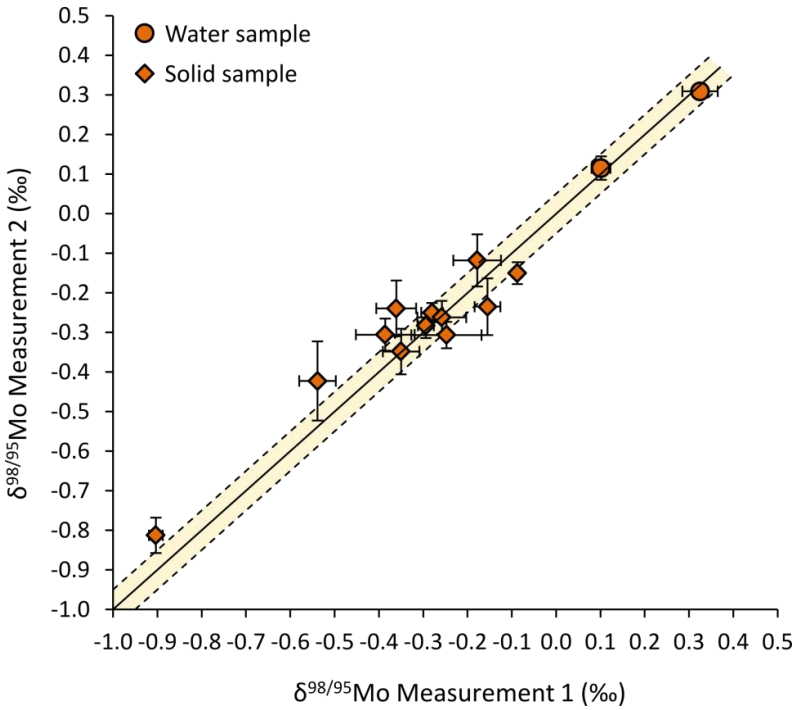

Figure S-4 Agreement between duplicate $\delta^{98/95}$Mo data for water and solid samples. Full procedural duplicates for a range of sediment samples are compared against a 1:1 line. The fits to the 1:1 line, indicated by dashed lines are for 0.05 ‰ deviations, which is the long term reproducibility on the BHVO-1 standard. Error bars indicated for measurements are ±2 SD on replicate runs of each individual sample.

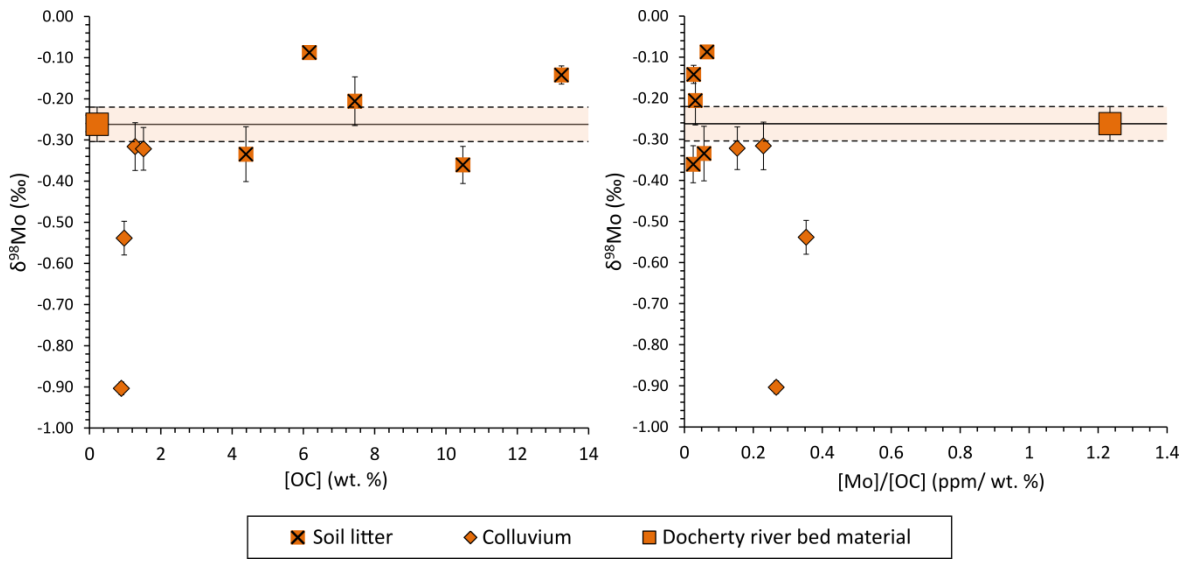

Figure S-5 Patterns in Mo distribution and composition in soils from the Alex Knob transect in the western Southern Alps, New Zealand (Table S-4). **A.** Relationship between the Mo isotope ratios and organic carbon concentration in soil materials. Surface soil litters are enriched in OC and have isotope ratios that are similar to the river bed material (horizontal line, $\delta^{98/95}$Mo = –0.26±0.04 ‰, ±2SD), while the colluvium samples have lower OC and lower $\delta^{98/95}$Mo values. **B.** Relationship between the Mo isotope ratios of soil materials and the relative abundance of Mo to organic carbon. Local river bed materials are dominated by Mo while soils are richer in organic matter, particularly in the case of the soil litters.

Supplementary Information References

Bezard, R., Fischer-Gödde, M., Hamelin, C., Brennecka, G. A., Kleine, T. (2016) The effects of magmatic processes and crustal recycling on the molybdenum stable isotopic composition of Mid-Ocean Ridge Basalts. *Earth and Planetary Science Letters* 453, 171-181.

Brookins, D.G. (1986) Rhenium as analog for fissiogenic technetium: Eh-pH diagram (25 C, 1 bar) constraints. *Applied Geochemistry 1*, 513-517.

Beaulieu, E., Goddéris, Y., Labat, D., Roelandt, C., Calmels, D., Gaillardet, J. (2011) Modeling of water-rock interaction in the Mackenzie basin: Competition between sulfuric and carbonic acids. *Chemical Geology* 289, 114-123.

Bouchez, J., Von Blanckenburg, F. and Schuessler, J.A. (2013) Modeling novel stable isotope ratios in the weathering zone. *American Journal of Science* 313, 267-308.

Calmels, D., Gaillardet, J., Brenot, A., France-Lanord, C. (2007) Sustained sulfide oxidation by physical erosion processes in the Mackenzie River basin: Climatic perspectives. *Geology* 35, 1003–1006.

Carson, M. A., Jasper, J. N., Conly, F. M. (1998) Magnitude and sources of sediment input to the Mackenzie Delta, Northwest Territories, 1974–94. *Arctic* 51, 116-124.

Dalai, T.K., Singh, S.K., Trivedi, J.R., Krishnaswami, S. (2002) Dissolved rhenium in the Yamuna River System and the Ganga in the Himalaya: Role of black shale weathering on the budgets of Re, Os, and U in rivers and CO_2 in the atmosphere. *Geochimica et Cosmochimica Acta* 66, 29-43.

Dellinger, M., Gaillardet, J., Bouchez, J., Calmels, D., Galy, V., Hilton, R.G., Louvat, P., France-Lanord, C. (2014) Lithium isotopes in large rivers reveal the cannibalistic nature of modern continental weathering and erosion. *Earth and Planetary Science Letters* 401, 359-372.

Galy, V., Bouchez, J., France-Lanord, C. (2007) Determination of total organic carbon content and $\delta^{13}C$ in carbonate-rich detrital sediments. *Geostandards and Geoanalytical research* 31, 199-207.

Gislason, S.R., Arnorsson, S., Armannsson, H. (1996) Chemical weathering of basalt in Southwest Iceland; effects of runoff, age of rocks and vegetative/glacial cover. *American Journal of Science* 296, 837-907.

Goldberg, S., Forster, H.S. (1998) Factors affecting molybdenum adsorption by soils and minerals. *Soil Science* 163, 109-114.

Goldberg, S., Lesch, S.M., Suarez, D.L. (2002) Predicting molybdenum adsorption by soils using soil chemical parameters in the constant capacitance model. *Soil Science Society of America Journal* 66, 1836-1842.

Goldberg, T., Gordon, G., Izon, G., Archer, C., Pearce, C.R., McManus, J., Anbar, A.D., Rehkämper, M. (2013) Resolution of inter-laboratory discrepancies in Mo isotope data: an intercalibration. *Journal of Analytical Atomic Spectrometry* 28, 724-735.

Greber, N.D., Siebert, C., Nägler, T.F., Pettke, T. (2012) $\delta^{98/95}$Mo values and molybdenum concentration data for NIST SRM 610, 612 and 3134: Towards a common protocol for reporting Mo data. *Geostandards and Geoanalytical Research* 36, 291-300.

Henderson, R.D., Thompson, S.M. (1999) Extreme rainfalls in the Southern Alps of New Zealand. *Journal of Hydrology (New Zealand)* 38, 309-330.

Hicks, D.M., Shankar, U., McKerchar, A.I., Basher, L., Lynn, I., Page, M., Jessen, M. (2011) Suspended sediment yields from New Zealand rivers. *Journal of Hydrology (New Zealand)* 50, 81-142.

Hilton, R.G., Gaillardet, J., Calmels, D., Birck, J.L. (2014) Geological respiration of a mountain belt revealed by the trace element rhenium. *Earth and Planetary Science Letters* 403, 27-36.

Hilton, R.G., Galy, V., Gaillardet, J., Dellinger, M., Bryant, C., O'Regan, M., Gröcke, D.R., Coxall, H., Bouchez, J., Calmels, D. (2015) Erosion of organic carbon in the Arctic as a geological carbon dioxide sink. *Nature* 524, 84-87.

Horan, K., Hilton, R.G., Dellinger, M., Tipper, E., Galy, V., Calmels, D., Selby, D., Gaillardet, J., Ottley, C.J., Parsons, D.R., Burton, K.W. (2019) Carbon dioxide emissions by rock organic carbon oxidation and the net geochemical carbon budget of the Mackenzie River Basin. *American Journal of Science* 319, 473-499.

Hovius, N., Stark, C.P., Allen, P.A. (1997) Sediment flux from a mountain belt derived by landslide mapping. *Geology* 25, 231-234.

Jacobson, A.D., Blum, J.D. (2003) Relationship between mechanical erosion and atmospheric CO_2 consumption in the New Zealand Southern Alps. *Geology* 31, 865-868.

Jacobson, A.D., Blum, J.D., Chamberlain, C.P., Craw, D., Koons, P.O. (2003) Climatic and tectonic controls on chemical weathering in the New Zealand Southern Alps. *Geochimica et Cosmochimica Acta* 67, 29-46.

Jonsdottir, J.F. (2008) A runoff map based on numerically simulated precipitation and a projection of future runoff in Iceland/Une carte d'écoulement basée sur la précipitation numériquement simulée et un scénario du futur écoulement en Islande. *Hydrological Sciences Journal* 53, 100-111.

Karimian, N., Cox, F.R. (1979) Molybdenum Availability as Predicted from Selected Soil Chemical Properties 1. *Agronomy Journal* 71, 63-65.

Kennedy, M.J., Chadwick, O.A., Vitousek, P.M., Derry, L.A., Hendricks, D.M. (1998) Changing sources of base cations during ecosystem development, Hawaiian Islands. *Geology* 26, 1015-1018.

King, E.K., Perakis, S.S., Pett-Ridge, J.C. (2018) Molybdenum isotope fractionation during adsorption to organic matter. *Geochimica et Cosmochimica Acta* 222, 584-598.

King, E.K., Thompson, A., Chadwick, O.A., Pett-Ridge, J.C. (2016) Molybdenum sources and isotopic composition during early stages of pedogenesis along a basaltic climate transect. *Chemical Geology* 445, 54-67.

Kim, Y.S., Zeitlin, H. (1968) The determination of molybdenum in seawater 1. *Limnology and Oceanography* 13, 534-537.

Li, Y., McCoy-West, A.J., Zhang, S., Selby, D., Burton, K.W., Horan, K. (2019) Controlling mechanisms for molybdenum isotope fractionation in porphyry deposits: the Qulong example. *Economic Geology* 114, 981-992.

Millot, R., Vigier, N., Gaillardet, J. (2010) Behaviour of lithium and its isotopes during weathering in the Mackenzie Basin, Canada. *Geochimica et Cosmochimica Acta* 74, 3897-3912.

McCoy-West, A. J., Chowdhury, P., Burton, K. W., Sossi, P., Nowell, G. M., Fitton, J. G., Kerr, A. C., Cawood, P. A., Williams, H. M. (2019) Extensive crustal extraction in Earth's early history inferred from molybdenum isotopes. *Nature Geoscience* 12, 946-951.

Mortimer, N. (2004) New Zealand's geological foundations. *Gondwana Research*, 7, 261-272.

Nägler, T.F., Anbar, A.D., Archer, C., Goldberg, T., Gordon, G.W., Greber, N.D., Siebert, C., Sohrin, Y., Vance, D. (2014) Proposal for an international molybdenum isotope measurement standard and data representation. *Geostandards and Geoanalytical Research* 38, 149-151.

Pearce, C.R., Cohen, A.S., Parkinson, I.J. (2009) Quantitative separation of molybdenum and rhenium from geological materials for isotopic determination by MC-ICP-MS. *Geostandards and Geoanalytical Research* 33, 219-229.

Pogge von Strandmann, P.A.E., Burton, K.W., James, R.H., van Calsteren, P., Gíslason, S.R., Mokadem, F. (2006) Riverine behaviour of uranium and lithium isotopes in an actively glaciated basaltic terrain. *Earth and Planetary Science Letters* 251, 134-147.

Rahaman, W., Goswami, V., Singh, S.K., Rai, V.K. (2014) Molybdenum isotopes in two Indian estuaries: Mixing characteristics and input to oceans. *Geochimica et Cosmochimica Acta* 141, 407-422.

Roser, B.P., Cooper, A.F. (1990) Geochemistry and terrane affiliation of Haast Schist from the western Southern Alps, New Zealand. *New Zealand journal of geology and geophysics* 33, 1-10.

Scheiderich, K., Helz, G.R., Walker, R.J. (2010) Century-long record of Mo isotopic composition in sediments of a seasonally anoxic estuary (Chesapeake Bay). *Earth and Planetary Science Letters* 289, 189-197.

Siebert, C., Pett-Ridge, J. C., Opfergelt, S., Guicharnaud, R. A., Halliday, A. N., Burton, K. W. (2015). Molybdenum isotope fractionation in soils: Influence of redox conditions, organic matter, and atmospheric inputs. *Geochimica et Cosmochimica Acta* 162, 1-24.

Tippett, J.M., Kamp, P.J. (1993) Fission track analysis of the late Cenozoic vertical kinematics of continental Pacific crust, South Island, New Zealand. *Journal of Geophysical Research: Solid Earth* 98, 16119-16148.

Torssander, P. (1989) Sulfur isotope ratios of Icelandic rocks. *Contributions to Mineralogy and Petrology* 102, 18-23.

Willbold, M., Elliott, T. (2017) Molybdenum isotope variations in magmatic rocks. *Chemical Geology* 449, 253-268.

Yang, J., Siebert, C., Barling, J., Savage, P., Liang, Y.-H., Halliday, A. N. (2015) Absence of molybdenum isotope fractionation during magmatic differentiation at Hekla volcano, Iceland. *Geochimica et Cosmochimica Acta* 162, 126-136.